

Monte Carlo simulation and dynamic scaling of surfaces in MBE growth

S. Pal and D. P. Landau

Center for Simulation Physics, The University of Georgia, Athens, Georgia 30602

(Received 11 August 1993; revised manuscript received 17 December 1993)

Film growth by molecular-beam epitaxy is modeled by a simple solid-on-solid model using Monte Carlo simulations. $L \times L$ substrates are used and both deposition and surface diffusion are allowed to occur simultaneously. Surface roughness is studied by measuring different surface characteristics: interface width, reflection high-energy electron-diffraction intensity, and kink density are calculated from configurations generated by simulation. We find a region of temperature and flux for which apparent layer-by-layer growth occurs. For long times, the interface width grows logarithmically with time, and its saturated value diverges logarithmically with substrate size. This unusual result suggests that within the context of this model all growing surfaces are asymptotically rough for infinite lateral extent. Because of the logarithmic behavior of the interface width, our model falls into the Edwards-Wilkinson universality class. The growth is intermediate between two-dimensional and three-dimensional nucleation and is experimentally observed in many epitaxial systems.

I. INTRODUCTION

The past two decades have been a period of remarkable advances in the growth of thin-film semiconductor structures.¹ Such progress has been possible mainly because of the advent of molecular-beam epitaxy (MBE) technology, which distinguishes itself from other vacuum deposition techniques by its much more precise control of beam fluxes, film thickness, and deposition conditions. Along with the development of MBE, the availability of sophisticated surface characterization techniques and surface analytical tools like scanning tunneling microscopy (STM) have made it possible to extract valuable information about a growing surface, and this has in turn stimulated the search for theoretical models of crystal growth. The morphology of a growing surface can be probed *in situ* using reflection high-energy electron diffraction (RHEED), and certain general features of the time dependence of the RHEED intensity are common to many experiments. At low temperatures the RHEED intensity drops smoothly as the film grows, signaling the creation of a smoothly growing, rough surface; but, as the temperature is raised, the overall intensity increases and begins to show oscillations² above some temperature known as the epitaxial temperature. The oscillations, which slowly decay with time, are interpreted as indicating increasingly imperfect layer-by-layer growth, i.e., surface roughness grows with successive layers. If the beam is temporarily stopped, the RHEED intensity recovers (interpreted as the recovery of flatness³), and it is thus a common practice to do “growth interrupt” to improve interfacial quality. The temperature at which oscillations are first observed in the RHEED intensity depends on the deposition rate; however, in experiments the substrate temperature is usually maintained between 300–800 °C in order to make device-quality layers. Such temperatures are low compared to the equilibrium roughening transition temperature,⁴ but sufficiently high to produce compact films.

Recent experiments have now succeeded in measuring surface roughness directly by scanning force microscopy.⁵

Because of the constant deposition of particles, the surface never has the opportunity to assume an equilibrium structure. MBE is thus a nonequilibrium process for which the “distance” from equilibrium is controlled by the substrate temperature and the incident flux. At any instant of time during growth, surface roughness is determined by competition between surface diffusion, which tries to flatten the surface, and deposition, which tends to make the surface rough. At the present time, however, we do not know how to express this “distance” from equilibrium in a sensible, quantifiable manner.

Effective efforts to understand the general features of MBE from a theoretical perspective began over a decade ago when Edwards and Wilkinson⁶ studied a simple model with both deposition and surface relaxation. A physical realization of their model is sedimentation of particles in a viscous fluid under the action of gravity. They derived an equation of the growing surface in order to study the evolution of the height-height correlations. Kardar, Parisi, and Zhang⁷ later proposed a more general growth equation by adding a new term to the Edwards-Wilkinson equation to account for lateral growth. Recently there have been numerous attempts to understand thin-film growth by simulation of computer models^{8–27} and by numerical solution of growth equations,^{28–35} analytical theories also have been developed to understand the nature of thin-film growth.^{36–42}

The study of surface roughness is not a new subject.⁴ Equilibrium behavior has already been studied by Monte Carlo simulations of SOS (solid-on-solid), DGSOS (discrete Gaussian solid-on-solid), and three-dimensional Ising models.^{43–45} Slightly more complicated systems have been studied as well.⁴⁶ In three dimensions there is a nonzero roughening temperature above which the surface produces steps freely, thus resulting in the rounding

of crystalline facets. Roughening has been experimentally observed⁴⁷ on vicinal (stepped) surfaces, and the early stages of roughening have been attributed to the meandering of steps rather than to spontaneous creation. Monte Carlo simulations have been carried out⁴⁸ to understand equilibrium roughening on vicinal surfaces; computer models⁴⁹ and numerical simulations of growth equations⁵⁰ have been used to understand roughening in growing vicinal surfaces. The question of a nonequilibrium roughening transition has also been addressed,⁵¹ and it is evident from the extensive literature that roughening is a very important problem. The numerical solution to growth equations has generally been aimed at determining the long-time behavior of growing interfaces, while MBE lattice simulations (except in Refs. 21 and 22) have been concerned mainly with determining microscopic details of MBE growth.

The purpose of the current study is to attempt to understand the basic properties of this growth from the perspective of statistical mechanics, i.e., the behavior of a large number of particles, rather than from employing a realistic but complicated model for which only systems of modest size can be used. We therefore do not attempt to describe material-dependent characteristics. To accomplish this we have carried out large-scale Monte Carlo simulations of a simple 2+1-dimensional model to determine the effects of competition between deposition and diffusion for different fluxes and temperatures. We have carefully examined the effects of finite lattice size and finite growth time. Preliminary results have been published elsewhere.⁵² In Sec. II we place this work in perspective by briefly reviewing previous theoretical and simulation work. In Sec. III we describe the model and the simulation method used, and in Sec. IV we present our results. We conclude in Sec. V.

II. BACKGROUND

To place the present work in context, we briefly review past theoretical and simulation studies of MBE growth. Perhaps the first successful attempt to treat randomly growing interfaces was by Hammersley (see Ref. 53), who used a stochastic cellular automaton to study growth of a film in d dimensions. Edwards and Wilkinson⁶ were the first to study a model with deposition and surface relaxation. Their approach to the problem is more applicable to our situation, and, although the problem has been treated quite differently in our case, we find the same type of dependence on system size of the steady-state height-height correlation functions.

In an attempt to describe the behavior of a growing surface from a phenomenological perspective, Villain²⁹ proposed a comprehensive growth equation that describes the evolution of the surface in the continuum limit

$$\frac{\partial H}{\partial t} = \nu \nabla^2 H + \lambda (\nabla H)^2 + K \nabla^2 (\nabla^2 H) + \sigma \nabla^2 (\nabla H)^2 + R + \xi, \quad (1)$$

where R is the renormalized deposition flux, ξ is the zero mean random fluctuation in the flux, and H is the height,

measured relative to the average height of the surface. Note that this equation contains the Edwards-Wilkinson (EW) equation,⁶ and the equation by Kardar, Parisi, and Zhang (KPZ),⁷ as special cases. By solving the growth equation with $\lambda=K=\sigma=0$, Edwards and Wilkinson showed that the steady-state and dynamic height-height correlation functions grow as $\ln(L)$ and $\ln(t)$, respectively. Guided by the ideas of universality, KPZ added a first-order, nonlinear term to the Edwards-Wilkinson growth equation to describe lateral growth, i.e., ($K=\sigma=0$). In models such as the Eden model⁵⁴ and the ballistic deposition model,⁵⁵ the KPZ equation provides a reasonable description of surface evolution in 1+1 dimensions. Other growth equations have been studied as well, where $\nu=\lambda=\sigma=0$,²⁷ $\nu=\lambda=0$,³³ and $\sigma=0$.³⁵

To characterize the universal behavior of growing interfaces, Family³⁶ studied dynamic scaling of rough surfaces in 1+1 dimensions, taking into account the effects of surface diffusion. It is generally accepted that the interface width satisfies the dynamic scaling equation⁵⁶

$$W(L, t) = L^\alpha F \left[\frac{t}{L^{\alpha/\beta}} \right] \quad (2)$$

for a system of lateral size L , where $z=\alpha/\beta$ is usually known as the dynamic exponent, and for the KPZ equation α and β satisfy the relation $\alpha+\alpha/\beta=2$. According to the dynamic scaling equation [Eq. (2)], the interface width grows with time as

$$W(L, t) \sim t^{1/2} \quad \text{for short times,} \quad (3)$$

$$W(L, t) \sim t^\beta \quad \text{for intermediate times,} \quad (4)$$

$$W(L, t \rightarrow \infty) \sim L^\alpha. \quad (5)$$

The exponents α and β characterize the scaling properties of the surface fluctuations for a given growth model and determine its universality class. In the ballistic deposition model, β is found to be $\frac{1}{3}$ in 1+1 dimensions whether surface relaxation is allowed or not. β is $\frac{3}{8}$ for the one-dimensional MBE growth model by Das Sarma and Tamborenea,²⁷ which agrees with the 1+1-dimensional lattice simulation by Wolf and Villain.²¹

In 2+1 dimensions $\beta=0$ for the Edwards-Wilkinson model, 0.22 for the Ballistic Deposition model, and $\frac{1}{4}$ for ballistic deposition with restructuring.⁵⁷ For a restricted SOS model by Kim and Kosterlitz,⁵⁸ β is found to be $\frac{1}{4}$ and $z=1.60$. Richards²² studied the steady-state behavior of the interface width in a model for which particles were allowed only to hop down, and the rate at which the steps were smoothed out was independent of step height. This model gave steady-state behavior similar to the Edwards-Wilkinson model. Although an exact solution of the KPZ equation is not available in 2+1 dimensions, numerical studies of the KPZ equation by Family⁵⁹ indicate that, when the nonlinear term is large, the value of α is close to the conjecture of Kim and Kosterlitz. When the nonlinear term is very small, the interface width grows very slowly with time, possibly indicating a logarithmic behavior, and when the nonlinear term is absent the exact solution to the Edwards-Wilkinson

equation is obtained. This observation suggests that dynamic scaling in accordance with Eq. (2) will be satisfied in models where the nonlinear term is large, but eventually there will be a crossover to the Edwards-Wilkinson regime when this term is small. In this paper we develop a scaling theory in that regime.

III. MODEL AND METHOD

We consider a solid-on-solid model growing on an $L \times L$ square lattice substrate with periodic boundary conditions. $h(\mathbf{r}, t)$ represents the height of the surface above the two-dimensional substrate at position \mathbf{r} and time t . Particles are deposited randomly on the surface at a constant rate, and deposition of a single particle at position \mathbf{r} increments the height by unity. The time scale can be related to a physical time scale in the following way: deposition of L^2 particles per Monte Carlo time unit corresponds to the growth of one layer per second for a system with a lattice constant of 10 \AA and a flux of $10^{14}/\text{cm}^2 \text{ sec}$. Typical values of the flux actually used in the simulations are between $10^{14}/\text{cm}^2 \text{ sec}$ and $10^{10}/\text{cm}^2 \text{ sec}$. In a single time step a small number of particles are deposited randomly on the surface, and then particles on the surface are allowed to hop to nearest-neighbor sites.

In principle, each particle on the surface can hop with probability P , and thus each particle should be tested. For very low hopping probabilities a different procedure is used to reduce the computer time needed: only some fraction f of the sites (randomly chosen) is actually allowed to hop, but with probability P/f . The size of the time step, i.e., the number of particles deposited, the probability P , and the fraction of particles allowed to hop in a given time step, are adjusted with temperature and deposition rate to avoid any systematic errors. This results in significant speed up of the computer program, thus enabling us to do large-scale simulations of the long-time behavior of MBE growth. The thermally activated hopping probability is given by the equation

$$P_{\text{hop}} = e^{-E_A/k_b T}, \quad (6)$$

where $E_A = nJ$ is a site-dependent activation energy, J is the "effective" bond energy, and n is the number of nearest neighbors. Note that J is not actually the physical total bond energy on a perfect lattice but is rather some effective value that results dynamically from correlated motions of the neighbors.

After breaking bonds, a particle that undergoes diffusion moves to a nearest-neighbor column subject to the restriction that its final position is not higher than the initial one. The probability for a particle to move to the k th nearest-neighbor site (assuming that it is empty) is given by

$$P^k = \frac{e^{-E^k/k_b T}}{\sum_i^m e^{-E^i/k_b T}}, \quad (7)$$

where m is the number of available sites and E^i is the site

energy available at the i th site. Thus the probability is highest for the particle to jump to that site, providing it with the highest coordination. Surface evaporation is not allowed, and this restriction limits the maximum temperature for which the results have physical relevance. Since we have only allowed the particles to hop down, we have effectively suppressed defect excitations, and the system has access only to those states that will tend to minimize the interfacial free energy. One can show that, for the temperatures of MBE growth and for the realistic values of bond energy and creation entropy of defects, the probability of defect formation is extremely small.

To allow studies of the statistical properties of an evolving interface, growth must proceed to very long times so that a scale-invariant state has been reached in which the surface has developed large-scale (long-wavelength) structures. In the long-time regime the surface is expected to have long-wavelength fluctuations, so in the steady state the microscopic details of the interactions are no longer important to the interface. Effective interactions between particles are then sufficient to reproduce the correct deformations in the surface.

Simulations have been carried out for $20 \leq L \leq 1000$, with the number of layers grown varied from run to run. Multiple growth runs have been made for the same parameters but with different random number sequences, and the results have been averaged together to reduce statistical fluctuations. For the longest single run, 250 different runs have been averaged together for $L = 200$, with 2500 layers growth for each run. This corresponds to adding a total of 2.5×10^{10} particles.

It is well known that random number sequences may have hidden correlations,⁶⁰ which could in turn introduce unwanted correlated movements of adatoms and thus spurious behavior of the shape and size of clusters. We implemented a minimal standard random number generator that is a prime-modulus multiplicative linear congruential generator⁶¹⁻⁶³ with multiplier 16 807 and a prime modulus of $2^{31} - 1$. No "unusual" patterns have been seen in surface projections, and comparison with data generated using other random number generators showed no obvious differences. "Snapshots" of the surface were generated using a Silicon Graphics (Indigo) graphics station. All the results presented in this paper have been performed on a cluster of IBM RS/6000 work stations. Vectorization of the algorithm is nontrivial due to the double stochasticity of deposition and diffusion.

To characterize the quality of the growing surface, we measured the interface width $W(L, t)$, RHEED intensity I , and kink density D from the configurations produced by the simulation. If $h(\mathbf{r}, t)$ is the height of the surface at position \mathbf{r} and time t , measured from the flat substrate, then the interface width is

$$W(L, t) = [\langle h^2(\mathbf{r}, t) \rangle - \langle h(\mathbf{r}, t) \rangle^2]^{1/2}, \quad (8)$$

where the thermal averages $\langle h^n \rangle$ are calculated via

$$\langle h^n(\mathbf{r}, t) \rangle = \frac{1}{L^2} \sum_{\mathbf{r}} h^n(\mathbf{r}, t). \quad (9)$$

Here the overbar denotes an average over the statistically

independent runs. The kink density D is defined as the number of kink sites per unit area. The RHEED intensity is calculated by a method given in Ref. 64. Denoting c_i as the coverage of the i th layer above the highest fully filled layer, the intensity of scattering in the out-of-phase condition from the first five layers (at any instant of time) is given as

$$I = G_0 \left[\sum_{i=1}^5 c_i^2 - 2 \sum_{i=1}^4 c_i c_{i+1} + 2 \sum_{i=1}^3 c_i c_{i+2} - 2 \sum_{i=1}^2 c_i c_{i+3} + 2 c_1 c_5 \right] + 4G_1 \sum_{i=1}^4 c_i c_{i+1} + 4G_3 \sum_{i=1}^2 c_i c_{i+3}, \quad (10)$$

where G_0 , G_1 , and G_3 are instrument response functions. (On the short-time scales for which we measured the RHEED intensity, we found no configuration with more than five layers above the highest completely filled layer.) The sensitivity of the RHEED intensity to the surface structure can be improved by adjusting the instrumental response functions. Wide response functions (i.e., G_1 , and G_3 comparable to G_0) would obscure the diminishing of the diffracted intensity by steps. For our measurements we assumed that $G_1 = G_3 = 0.025G_0$. This procedure is sensitive to the coverage of the surface, but does not give any information about the compactness of clusters.

IV. RESULTS

A. Short-time behavior

The analysis of a growing surface can be broadly divided into three categories, namely its behavior at short, intermediate, and long times. Figure 1 shows a plot of interface width W versus time t for relatively short times. For very early times the width is independent of temperature and consistent with an increase as $t^{1/2}$, in agreement with Ref. 56. This behavior is a trivial consequence of

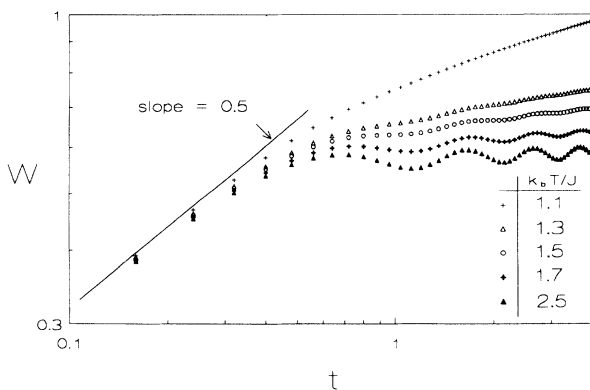


FIG. 1. Time dependence of surface width W at short times for $L = 800$, flux $= 10^{14}/\text{cm}^2 \text{sec}$, and different values of $k_b T/J$, where J is the effective bond energy. Data points are from averages over 15 different runs.

the sequential adsorption of particles on an essentially flat surface. The time dependence of the width then changes fairly rapidly and begins to show oscillations as the temperature increases. Although we have not presented any results at a different flux, it is not difficult to see that such behavior will be independent of flux, too, since it arises because of the absence of correlations among particles at very short times. When nucleation commences on the surface, correlations appear and the mean width increases as

$$W(L, t) \sim \ln(t) \quad \text{for } \tau_i \ll t \ll \tau_c, \quad (11)$$

where τ_i is the induction time, i.e., the time taken for the initial transients to damp out, and τ_c is the time taken for the interface width to saturate.

Figure 2 shows a semilog plot of interface width versus time for $k_b T/J = 1.7$ and flux $= 10^{14}/\text{cm}^2 \text{sec}$. Although oscillations are clearly seen, the mean value of the width evolves as $\log_{10}(t)$ over a range of time that begins at less than $t = 1$ sec and extends all the way to $t = 20$ sec. A comparison of the time dependence of the surface width W , RHEED intensity I , and kink density D for a range of different temperatures is shown in Fig. 3. At high temperatures the width shows oscillations that vanish as the temperature is decreased. These oscillations indicate layer-by-layer growth, and the increase of the interfacial width with time indicates evolution of surface roughness. One can see striking similarities between experimental⁶⁵ and simulation results for the effect of growth interrupt on the RHEED intensity. In this model we have allowed the particles only to hop down the step edge; thus the equilibrium interface width would be zero at all temperatures. This restriction is certainly not physical at high temperatures, where the surface will tend to create defects spontaneously; but at MBE temperatures, particularly around the epitaxial temperature, this assumption is realistic. If the particles are allowed to hop both up and down a step edge, the equilibrium interfacial width is nonzero. We have measured the equilibrium interface width in a separate simulation for a fixed lattice size, and for comparison these values are indicated by arrows in

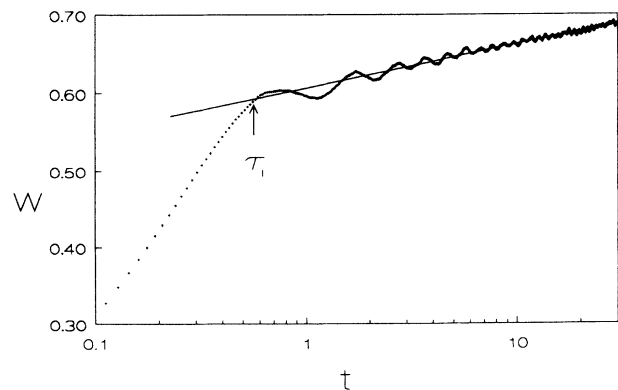


FIG. 2. Semilogarithmic plot of surface width W vs time for $L = 1000$, $k_b T/J = 1.70$, and flux $= 10^{14}/\text{cm}^2 \text{sec}$. Data are averages over five different runs. The position of the arrow shows the approximate location of the induction time τ_i .

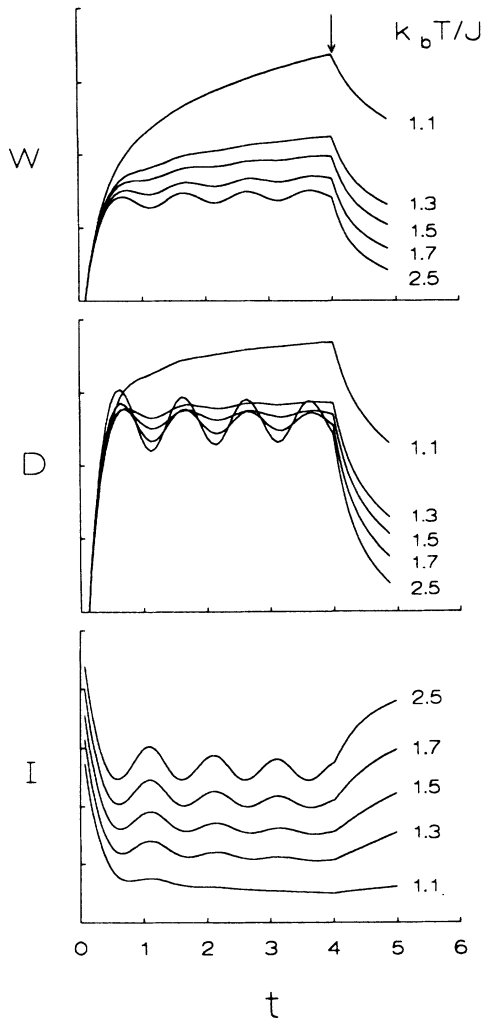


FIG. 3. Time dependence of surface width W , kink density D , and RHEED intensity I for $L = 800$, flux = $10^{14}/\text{cm}^2 \text{ sec}$, and different values of $k_b T/J$. Data represent averages over 15 different runs. The position of the arrow indicates when the flux was turned off.

Fig. 4 at the corresponding temperatures. Note that the equilibrium values show the opposite temperature dependence compared to the values of the width when the surface is far from equilibrium.

There are mainly two rates in the system: (1) the rate for surface processes to occur R_{sd} (mainly surface diffusion), and (2) the deposition rate R_f . One can observe very different growth modes depending on the ratio of R_{sd}/R_f . Thus, by appropriately adjusting R_f , it is possible to obtain epitaxial growth at room temperature.⁶⁶ For true layer-by-layer growth to occur, each layer must be completely filled before a new layer can grow; however, in the context of our model, we will show that such a condition is never achieved.

To better understand the manner in which growth proceeds, we generated pictures of the surface at a series of different times. Figure 5 shows a sequence of snapshots of a growing surface for a near-layer-by-layer

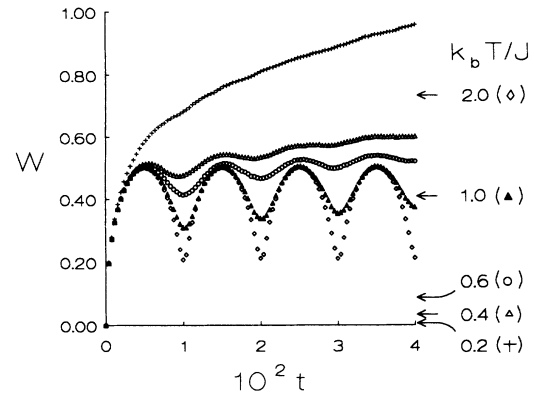


FIG. 4. Time dependence of surface width W for $L = 100$, Flux = $10^{12}/\text{cm}^2 \text{ sec}$, and a variety of $k_b T/J$. Data represent averages over 20 different runs. The position of the arrows indicate the value of the equilibrium interface width at the corresponding temperature. Note that the time scale is 100 times larger than in the case of flux = $10^{14}/\text{cm}^2 \text{ sec}$, implying a direct dependence of growth rate on flux, since desorption is absent.

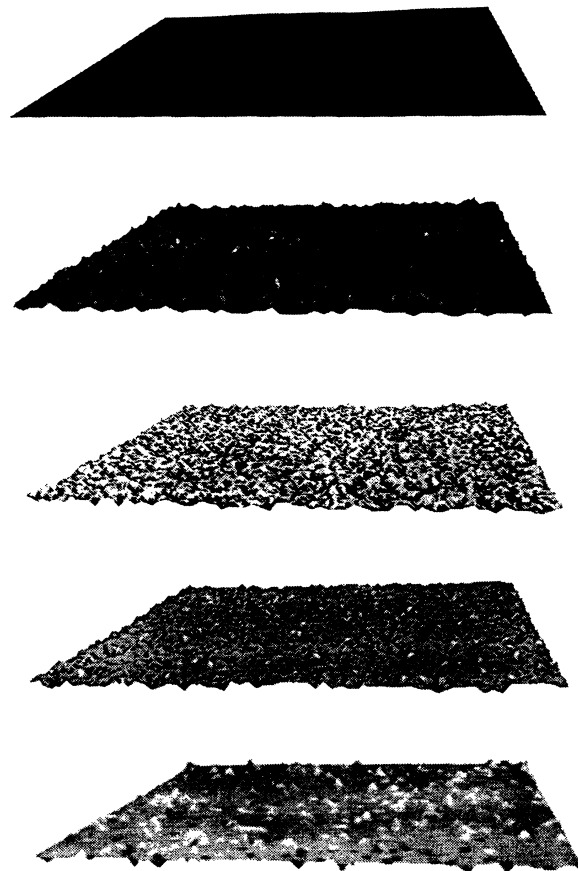


FIG. 5. Sequence of snapshots of a growing surface at different coverages (top to bottom) 0.0, 0.25, 0.50, 0.75, and 1.00. The simulation parameters are $L = 128$, $k_b T/J = 2.50$, and flux = $10^{13}/\text{cm}^2 \text{ sec}$. Lighter areas are at a greater height above the substrate than dark areas.

growth mode. The small size of the islands and the overall fractal-like appearance of the surface structure are a sign of high surface energy, and suggests that the surface is far from equilibrium. By changing the flux and temperature appropriately, it is possible to grow a surface that is near equilibrium. Such surfaces are characterized by large compact islands (Fig. 6). One of the advantages of visual examination of the computed surface is that it gives an idea how a real surface might look during growth. Observation of a growing surface in experiments is difficult technically, and RHEED is the only *in situ* technique available to probe surface features. To observe experimentally by STM how the surface looks *during the growth process*, the system has to be immediately quenched when the flux is turned off. Otherwise the surface would relax into equilibrium and exhibit a substantially different structure, depending on the flux and substrate temperature.

In Fig. 7(a) we show a picture of a surface grown with a flux of $5 \times 10^{12}/\text{cm}^2\text{sec}$ and at a temperature of $k_b T/J = 0.7$, up to a coverage of 0.25, at which point the flux is turned off. We then quenched this surface down to $k_b T/J = 0.5$, and allowed it to relax for 10 sec. The resulting configuration is shown in Fig. 7(b). One can see a large difference in cluster density between Figs. 7(a) and 7(b). Mo *et al.*⁶⁷ measured the island number density by STM for homoepitaxy on a Si(001) surface, and compared this density to the growth patterns generated by a simulated model to obtain the attempt frequency R_0 and the activation energy E_A for Si. This method yielded impressive values for the measured quantities, given that a very

simple simulation model was used. Recently, the effect of growth interruption has been studied experimentally using STM on a GaAs(001) surface.⁶⁸ Our simulation results agree qualitatively with that experiment.

B. Long-time results

It has been experimentally observed that during MBE growth the surface roughness increases as growth proceeds, resulting in a decaying RHEED intensity. To gain insight into the cause of this surface roughness, we must understand the behavior of an interface grown for a very long time such that the growth dynamics have transformed the interface width to a spatially and temporally scale-invariant state. We can interpret the surface diffusion and incident flux as two noise sources in a MBE system that produce fluctuations in the interface width. The noise is eventually eliminated by averaging over many different conformations of the growing surface. The diffusion tends to minimize surface deformations (far below the equilibrium roughening temperature), while the flux tends to build up surface deformations (fluctuations). The relative strength of these two noises determines the amplitude of the surface fluctuations. Only the long-wavelength modes of these fluctuations persist at long times, and this drives the system to a self-organized state.

To demonstrate how the surface fluctuations grow with time, we show snapshots of the growing surface (Fig. 8) for $t \gg \tau_i$. At this point, the initial transients have damped out or, equivalently, the adatoms have nucleated

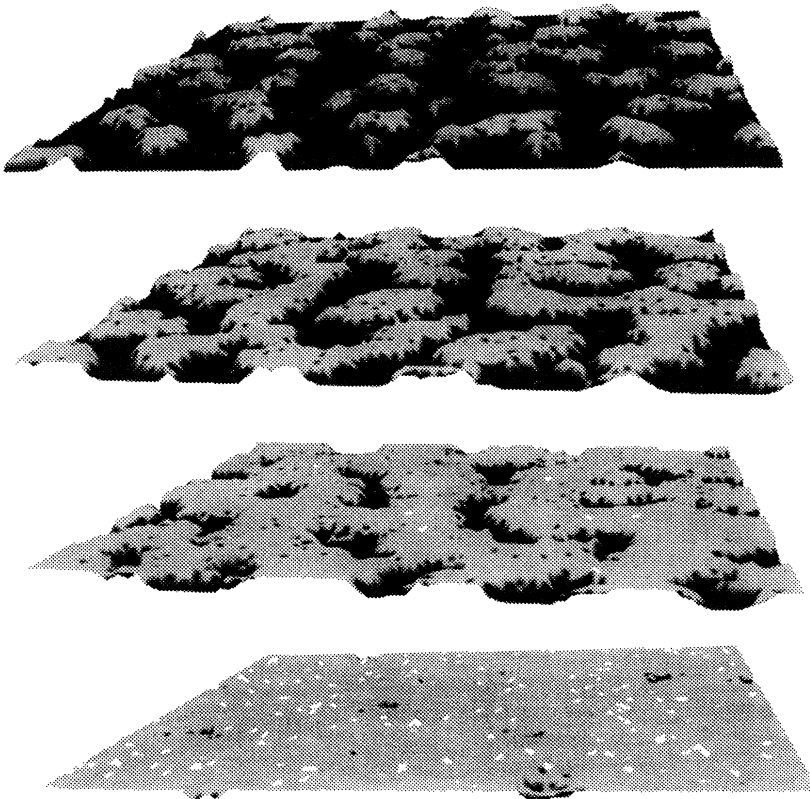


FIG. 6. Sequence of snapshots of growing surfaces for a much smaller flux than in Fig. 5 at coverages (top to bottom) 0.25, 0.50, 0.75, and 1.00. Simulation parameters are $L = 128$, $K_b T/J = 0.70$, and flux = $10^{10}/\text{cm}^2\text{sec}$.

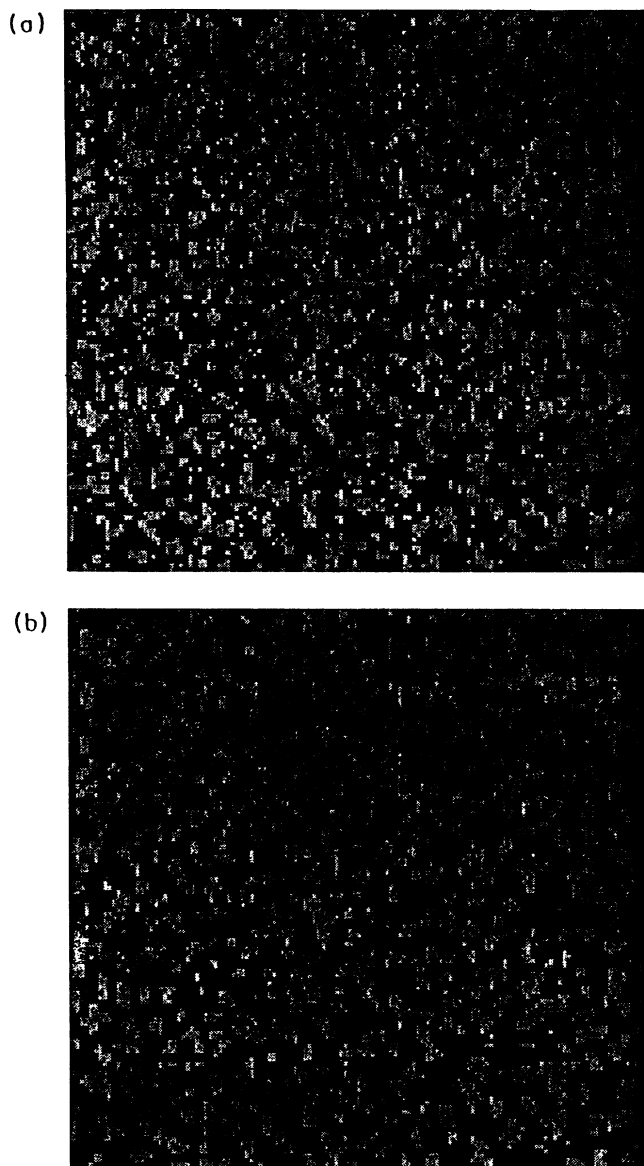


FIG. 7. (a) Surface growth at $k_b T/J=0.7$, flux $=5 \times 10^{12}/\text{cm}^2 \text{ sec}$, and coverage of 0.25. Light areas indicate the adatoms. (b) The surface shown in this figure is first grown up to a coverage of 0.25 with the same simulation parameters as in (a). The flux is then turned off, and the surface is quenched to a temperature of $k_b T/J=0.5$. The picture shown here is taken 10 sec after the quenching.

to form clusters such that the longest wavelength is much larger than the lattice constant. At $t=600$ sec the interface width has already reached saturation, and the picture shows that the most dominant mode on the surface has the longest wavelength. The long-time results for the interface width are shown in Fig. 9. To understand the results in Fig. 9, we note that there are two correlation lengths in the system, one perpendicular and the other parallel to the substrate.⁶⁹ On a growing surface, these correlations would grow indefinitely for an infinitely large

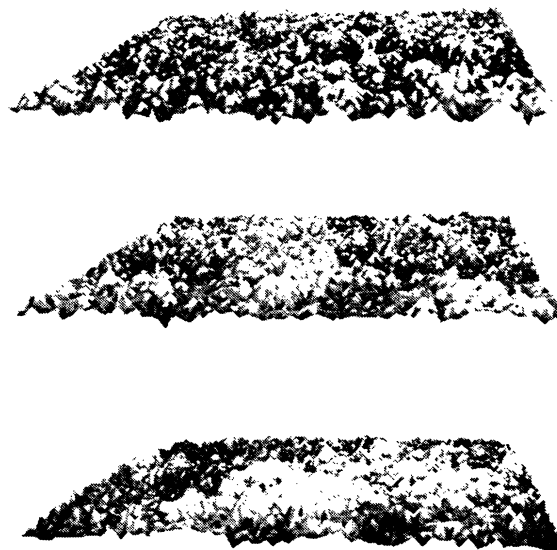


FIG. 8. Growth of surface fluctuations with time is shown in these pictures. The snapshots are taken at times (top to bottom) $t=10, 20$, and 600 sec. The interfacial width saturated around $t=300$ sec. The lattice size is $L=128$, $k_b T/J=1.70$, and flux $=10^{14}/\text{cm}^2 \text{ sec}$.

system.⁵² Note that in a real system, the correlations become constrained due to the finite grain size of the deposited material. From our simulation results (Fig. 10) we find $W(L, t \rightarrow \infty) = W_0 (\ln L)^\delta$, where δ depends in general on flux and temperature. From the analysis of the scaling plot in Fig. 10, we find the empirical relation

$$W(L, t \rightarrow \infty) = W_0 \exp[(J/k_b T)^\mu \ln(\ln L)^\phi], \quad (12)$$

where $W_0 = 0.50 \pm 0.02$, $\mu = 1.67$, and $\phi = 0.48 \pm 0.03$, implying $\delta = \phi(J/k_b T)^\mu$. At a given temperature, if the flux is changed, the interface width also changes. This offset in the width can be nullified by appropriately adjusting

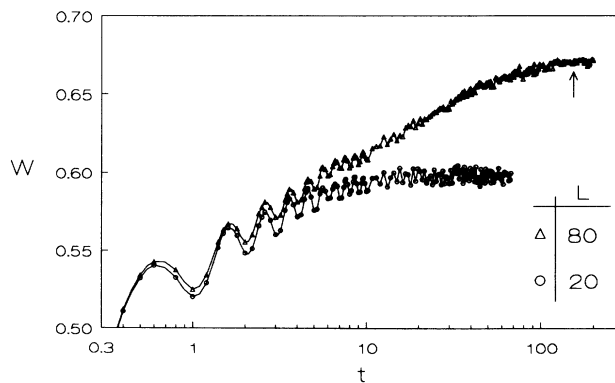


FIG. 9. Long-time behavior of the surface width W for different lattice sizes L at $k_b T/J=1.20$ and flux $=5 \times 10^{12}/\text{cm}^2 \text{ sec}$. The approximate location of the saturation time for $L=80$ is shown by the arrow. The line through the data points is a guide to the eye, and clearly shows the oscillations in the interface width.

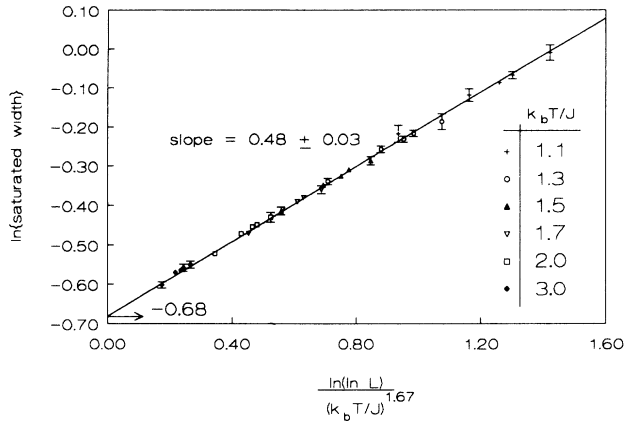


FIG. 10. Scaling plot of the saturated interface width $W(L, t \rightarrow \infty)$ for various lattice sizes L and different temperatures $k_b T/J$. Flux = $10^{14}/\text{cm}^2 \text{sec}$. A line drawn through the data intercepts the y axis at -0.68 , as denoted by the arrow.

the temperature. We expect Eq. (12) to be valid at all fluxes for which apparent layer-by-layer growth is observed, and μ can be regarded as the growth exponent that characterizes surface fluctuations with temperature in the apparent layer-by-layer growth regime.

We now consider dynamic scaling at a single temperature. The time needed by the surface fluctuations to reach the order of the system size is τ_c , which has a power-law dependence on the system size, i.e., $\tau_c = b_0 L^z$, where z is the dynamic exponent. This leads us to define a dynamic scaling equation

$$W(L, t) = W_0 (\ln L)^\delta \mathcal{F} \left[\frac{t}{\tau_c(L)} \right], \quad (13)$$

where

$$\mathcal{F} \left[\frac{t}{\tau_c(L)} \right] = 1 \quad \text{for } t \gg \tau_c, \quad (14)$$

$$\mathcal{F} \left[\frac{t}{\tau_c(L)} \right] \propto \ln \left[\frac{t}{\tau_c(L)} \right] \quad \text{for } \tau_i \ll t \ll \tau_c. \quad (15)$$

At $k_b T/J = 1.50$ and a flux of $10^{14}/\text{cm}^2 \text{sec}$, we obtain $\delta = 0.25 \pm 0.02$, $b_0 = 0.082 \pm 0.002$, and $z = 1.61 \pm 0.02$. Note that a comparison of Eqs. (13) and (2) gives us $\alpha = 0$ and $\beta = 0$. Thus, the relation $\alpha + \alpha/\beta = 2$ is not applicable for our model. However, α/β approaches some limiting value z that sets the time scale for the crossover to the scale-invariant state. In other 2+1-dimensional models, the value of z has been found to be 1.6 to 1.7.^{58,70-75} The plot of scaled width $\mathcal{W} = W(L, T)/W_0 (\ln L)^\delta$ versus scaled time t/τ_c is shown in Fig. 11. We see that scaling is obeyed nicely in the limit of large system sizes. Note that the scaling of data was attempted at a different temperature than in Ref. 52. We expect this scaling form to hold when the temperature is not too high or too low. This unusual scaling result suggests that, within the context of this model, the surface width diverges for an

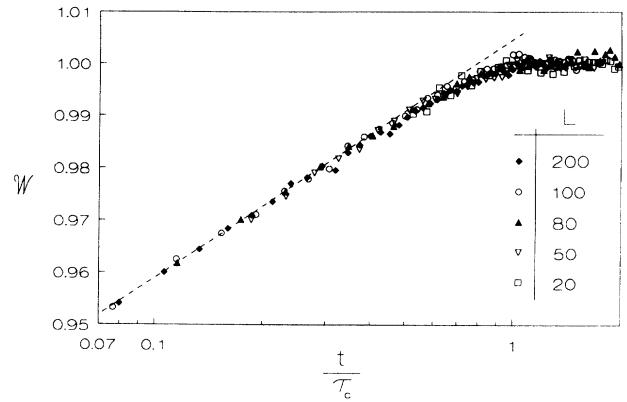


FIG. 11. Dynamic scaling plot for different lattice sizes at $k_b T/J = 1.50$, and flux = $10^{14}/\text{cm}^2 \text{sec}$. The region where oscillations in the interface width are observed has been smoothed out by using average values over a time interval of $\Delta t \approx 1 \text{ sec}$. The scaled width is $\mathcal{W} = W(L, t)/W_0 (\ln L)^\delta$, and the scaled time is t/τ_c , where $\tau_c = b_0 L^z$. The plot is for $W_0 = 0.50$, $\delta = 0.251$, $b_0 = 0.082$, and $z = 1.61$. Note that the time axis is logarithmic, showing the consistency of the data with a logarithmic scaling function.

infinitely large substrate. Hence no growing surface can be “ideally” smooth. Note that, if the flux is weak, the deformations in the surface have extremely large wavelengths; thus, to obtain the correct size effects, the system size in a simulation has to be at least the size of the longest wavelength.

From the scaling results we conclude that our system can be described by the Edwards-Wilkinson equation. To understand the origin of the logarithmic behavior in our model, we see that in the Edwards-Wilkinson equation such behavior arises because of the term $\nabla^2 h$, which tries to reduce the absolute local curvature at each point $h(\mathbf{r})$ on the surface, i.e., it tries to make the surface growth two dimensional. In our model at very low temperatures the growth is totally three dimensional, and the width is expected to scale as

$$W(L, t \rightarrow \infty) \sim L^\alpha, \quad (16)$$

in agreement with the analysis by Family.⁵⁶ As the temperature is increased, the three-dimensional character of the growth is lost by the activated hopping of adatoms, and growth proceeds via two-dimensional nucleation of successive layers. Above the epitaxial temperature three-dimensional islanding still persists, but growth proceeds mainly by two-dimensional spreading. This is responsible for the logarithmic character of growth. Hence the most general scaling equation (for growth with surface diffusion) for the interface width should be

$$W(L, t \rightarrow \infty) \sim L^\alpha (\ln L)^\delta, \quad (17)$$

where $\delta \rightarrow 0$ as the temperature goes to zero and $\alpha \rightarrow 0$ as the temperature is increased. Above the epitaxial temperature the correction to scaling comes from the term L^α , and the amount of correction depends on the value of temperature and flux at which the simulation is done. A

striking similarity exists between a growing MBE system and the sedimentation model of Edwards and Wilkinson. Since growth starts from an initially flat substrate, the average number of bonds available at each nucleation site is highest in the layer closest to the substrate and lowest in the topmost layer. This creates a downhill attraction. In the Edwards-Wilkinson model there is a gravitational potential gradient, and hence the particles move downhill to the lowest possible height; in a MBE system particles prefer to move downhill to the highest-coordinated site to minimize the step free energy. A similar explanation of this downhill motion has been given by Kessler and Orr.³⁴ In an equilibrium system, atoms hop up and down the step edge and the net current is zero. In a MBE system the adatom concentration is supersaturated because the incident flux keeps supplying particles on the terraces. Because of the difference in adatom concentration between the layers, there is a net downward current of adatoms that travels down the hill to increase coordination. Recently, surface diffusion currents have been measured in a simulation for a variety of one- and two-dimensional solid-on-solid models.²⁵ A downhill current is produced in the asymptotic regime of the Wolf and Villain model (WV),²¹ and Edwards-Wilkinson behavior is observed after the system crosses over a characteristic time scale. The observation of Edwards-Wilkinson behavior after a characteristic time scale is consistent with our simulations. Krug, Plischke, and Siegert²⁵ also find that a downhill current produces a stable surface, which is required for epitaxy. This observation supports our conclusion that ideal MBE growth must belong to the Edwards-Wilkinson universality class.

V. CONCLUSIONS

Using a simple solid-on-solid model that includes both deposition and surface diffusion, we recover the general features of MBE growth. The pictures of the growing surfaces are helpful in understanding the nature of MBE growth, and show that in a nonequilibrium condition the

growing islands have fractal-like structures. When growth proceeds in a thermodynamic condition that is not too far from equilibrium, the islands are compact, and growth occurs predominantly by step flow. In this case, the islands are large and uniformly shaped. The surface pictures are most interesting in the long-time regime where large-scale structures develop. The pictures explicitly show the saturation of the interface width when surface fluctuations cannot increase any more because of finite system size. We find a growth exponent of $\mu = 1.67$ from the scaling of long-time results for the interface width at different temperatures, while the dynamic scaling yields a dynamic exponent of $z = 1.61$. The dynamic scaling results of the interface width suggests that, within the context of this model, true layer-by-layer growth does not exist. Since the dynamic and steady-state height-height correlation functions have logarithmic behavior, our model falls within the Edwards-Wilkinson universality class. A surface growing by deposition and diffusion in 2+1 dimensions (under SOS restrictions) and the Edwards-Wilkinson model belong to the same universality class. In the former, particles tend to move downhill driven by the bond attraction to minimize step free energy; in the latter, particles travel downhill driven by gravitation to minimize potential energy. From the analysis of the Edwards-Wilkinson growth equation, we find that the logarithmic character of our model is caused by the characteristic two-dimensional spreading and three-dimensional islanding of thin films. This is similar to Stranski-Krastanov growth mode⁷⁶ and is observed in many epitaxially-growing systems.

ACKNOWLEDGMENTS

We are indebted to S. Follin for his expertise in the visualization of the surface structures produced by the simulations. We thank Burkhard Dünweg for his critical reading of the manuscript. This research was supported in part by NSF Grant No. DMR-9100692.

¹A. Y. Cho and J. R. Arthur, *Prog. Solid State Chem.* **10**, 157 (1975).

²T. Sakamoto, N. J. Kawai, T. Nakagawa, K. Ohta, and T. Kojima, *Surf. Sci.* **174**, 651 (1986).

³J. H. Neave, B. A. Joyce, P. J. Dobson, and N. Norton, *Appl. Phys. A* **31**, 1 (1983).

⁴W. K. Burton, N. Cabrera, and F. C. Frank, *Philos. Trans. Soc. (London)* **243A**, 299 (1951).

⁵M. A. Cotta, R. A. Hamm, T. W. Staley, S. N. G. Chu, L. R. Harriott, M. B. Panish, and H. Temkin, *Phys. Rev. Lett.* **70**, 4106 (1993).

⁶S. F. Edwards and D. R. Wilkinson, *Proc. R. Soc. London Ser. A* **381**, 17 (1982).

⁷M. Kardar, G. Parisi, and Y. Zhang, *Phys. Rev. Lett.* **56**, 889 (1986).

⁸G. H. Gilmer, *J. Cryst. Growth* **49**, 465 (1980).

⁹J. Singh and A. Madhukar, *J. Vac. Sci. Technol. B* **1**, 305

(1983).

¹⁰G. H. Gilmer and J. Q. Broughton, *J. Vac. Sci. Technol. B* **1**, 298 (1983).

¹¹A. Madhukar and S. Ghaisas, *CRC Critical Rev. Solid State Mater. Sci.* **14**, 1 (1988).

¹²S. A. Barnett and A. Rockett, *Surf. Sci.* **198**, 133 (1988).

¹³M. R. Wilby, S. Clarke, and D. D. Vvedensky, *Phys. Rev. B* **40**, 10 617 (1989).

¹⁴T. Kawamura, A. Kobayashi, and S. Das Sarma, *Phys. Rev. B* **39**, 12 723 (1989).

¹⁵W. M. Plotz, K. Hingerl, and H. Sitter, *J. Cryst. Growth* **115**, 186 (1991).

¹⁶S. Clarke, M. R. Wilby, and D. D. Vvedensky, *Surf. Sci.* **255**, 91 (1991).

¹⁷I. K. Marmorosk and S. Das Sarma, *Phys. Rev. B* **45**, 11 262 (1992).

¹⁸Z. Jiang and C. Ebner, *Phys. Rev. B* **45**, 6163 (1992).

- ¹⁹J. W. Evans, Phys. Rev. B **39**, 5655 (1989).
- ²⁰D. A. Faux, G. Gaynor, C. L. Carson, C. K. Hale, and J. Bernholc, Phys. Rev. B **42**, 2914 (1990).
- ²¹D. E. Wolf and J. Villain, Europhys. Lett. **13**, 389 (1990).
- ²²P. M. Richards, Phys. Rev. B **43**, 6750 (1991).
- ²³H. Metiu, Y. T. Lu, and Z. Zhang, Science **255**, 1088 (1992).
- ²⁴N. Haider, M. R. Wilby, and D. D. Vvedensky, Appl. Phys. Lett. **62**, 3108 (1993).
- ²⁵J. Krug, M. Plischke, and M. Siegert, Phys. Rev. Lett. **70**, 3271 (1993).
- ²⁶D. A. Kessler, H. Levine, and L. M. Sander, Phys. Rev. Lett. **69**, 100 (1992).
- ²⁷S. Das Sarma and P. Tamborenea, Phys. Rev. Lett. **66**, 325 (1991).
- ²⁸D. A. Huse, J. G. Amar, and F. Family, Phys. Rev. A **41**, 7075 (1990).
- ²⁹J. Villain, J. Phys. I **1**, 19 (1991).
- ³⁰J. G. Amar and F. Family, J. Phys. I **1**, 175 (1991).
- ³¹P. Lam and F. Family, Phys. Rev. A **44**, 4854 (1991).
- ³²C. Lam and L. M. Sander, Phys. Rev. Lett. **69**, 3338 (1992).
- ³³Z. W. Lai and S. Das Sarma, Phys. Rev. Lett. **66**, 2348 (1991).
- ³⁴D. A. Kessler and B. G. Orr (unpublished).
- ³⁵L. Golubović and R. Bruinsma, Phys. Rev. Lett. **66**, 321 (1991).
- ³⁶A. K. Myers-Beaghton and D. D. Vvedensky, Surf. Sci. Lett. **240**, L599 (1990).
- ³⁷G. S. Bales and A. Zangwill, J. Vac. Sci. Technol. A **9**, 145 (1991).
- ³⁸M. Ozdemir and A. Zangwill, J. Vac. Sci. Technol. A **10**, 684 (1992).
- ³⁹M. C. Bartelt and J. W. Evans (unpublished).
- ⁴⁰A. A. Wheeler, C. Ratsch, A. Morales, H. M. Cox, and A. Zangwill, Phys. Rev. B **46**, 12 675 (1992).
- ⁴¹T. Hwa, M. Kardar, and M. Paczuski, Phys. Rev. Lett. **66**, 441 (1991).
- ⁴²D. G. Stearns, Appl. Phys. Lett. **62**, 1745 (1993).
- ⁴³R. H. Swendsen, Phys. Rev. B **15**, 5421 (1977).
- ⁴⁴R. H. Swendsen, Phys. Rev. B **18**, 492 (1978).
- ⁴⁵K. K. Mon, D. P. Landau, and D. Stauffer, Phys. Rev. B **42**, 545 (1990).
- ⁴⁶F. Schmid and K. Binder, Phys. Rev. B **46**, 13 565 (1992).
- ⁴⁷E. H. Conrad, R. M. Alten, D. S. Kaufman, L. R. Allen, T. Engel, M. Nijs, and E. K. Reidel, J. Chem. Phys. **84**, 1015 (1986).
- ⁴⁸T. N. Einstein, T. M. Jung, N. C. Bartelt, E. D. Williams, and C. Rottman, J. Vac. Sci. Technol. A **10**, 2600 (1992).
- ⁴⁹D. E. Wolf, Phys. Rev. Lett. **67**, 1783 (1991).
- ⁵⁰K. Moser and D. E. Wolf, in *Surface Disordering: Growth, Roughening and Phase Transitions (Les Houches Proceedings)*, edited by R. Jullien *et al.* (Nova Science, Commack, NY, 1992).
- ⁵¹R. Kariotis, J. Phys. A **22**, 2781 (1989).
- ⁵²S. Pal and D. P. Landau, in *Computer Aided Innovation of New Materials II*, edited by M. Doyama, J. Kihara, M. Tonaoka, and R. Yamamoto (Elsevier, Amsterdam, 1993), p. 371.
- ⁵³J. M. Hammersley, in *Proceedings of the Fifth Berkeley Symposium on Mathematical Statistics and Probability*, edited by L. Le Cam and J. Neyman (University of California Press, Berkeley, 1967), pp. 89–117.
- ⁵⁴M. Eden, in *Proceedings of the Fourth Berkeley Symposium on Mathematical Statistics and Probability*, edited by J. Neyman (University of California Press, Berkeley, 1961), Vol. 4, pp. 223–239.
- ⁵⁵P. Meakin, P. Ramanlal, L. M. Sander, and R. C. Ball, Phys. Rev. A **34**, 5091 (1986).
- ⁵⁶F. Family, J. Phys. A **19**, L441 (1986).
- ⁵⁷R. Jullien and P. Meakin, Europhys. Lett. **4**, 1385 (1987).
- ⁵⁸J. M. Kim and J. M. Kosterlitz, Phys. Rev. Lett. **62**, 2289 (1989).
- ⁵⁹F. Family, in *Dynamical Phenomena at Surfaces, Interfaces, and Membranes*, Les Houches Lecture Series, edited by D. Beysens, G. Forgacs, and N. Boccara (Nova Science, Commack, NY, 1991).
- ⁶⁰A. M. Ferrenberg, D. P. Landau, and Y. J. Wong, Phys. Rev. Lett. **69**, 3382 (1992).
- ⁶¹P. Bratley, B. L. Fox, and E. L. Schrage, *A Guide to Simulation* (Springer-Verlag, New York, 1983), pp. 180–213.
- ⁶²A. M. Law and W. D. Kelton, *Simulation Modeling and Analysis* (McGraw-Hill, New York, 1982), pp. 219–213.
- ⁶³*Computer Performance Modeling Handbook*, edited by S. S. Lavenberg (Academic, New York, 1983), pp. 223–229.
- ⁶⁴C. S. Lent and P. I. Cohen, Surf. Sci. **139**, 121 (1984).
- ⁶⁵P. J. Dobson, B. A. Joyce, J. H. Neave, and J. Zhang, J. Cryst. Growth **81**, 1 (1987).
- ⁶⁶D. J. Eaglesham, H. J. Gossmann, and M. Cerullo, Phys. Rev. Lett. **65**, 1227 (1990).
- ⁶⁷Y. W. Mo, J. Kleiner, M. B. Webb, and M. G. Lagally, Phys. Rev. Lett. **66**, 1998 (1991).
- ⁶⁸T. Ide, A. Yamashita, and T. Mizutani, Surf. Sci. **287/288**, 1013 (1993).
- ⁶⁹F. Family, Physica A **168**, 561 (1990).
- ⁷⁰D. E. Wolf and J. Kertesz, Europhys. Lett. **4**, 651 (1987).
- ⁷¹T. Halpin-Healy, Phys. Rev. A **42**, 711 (1990).
- ⁷²B. M. Forrest and L. H. Tang, Phys. Rev. Lett. **62**, 442 (1989).
- ⁷³J. M. Kim, M. A. Moore, and A. J. Bray, Phys. Rev. A **44**, 2345 (1991).
- ⁷⁴M. Schwartz and S. F. Edwards, Europhys. Lett. **20**, 301 (1992).
- ⁷⁵J. P. Bouchaud and M. E. Cates, Phys. Rev. E **47**, R1455 (1993); **E 48**, 635(E) (1993). Note that d in this paper refers to the dimensionality of the interface.
- ⁷⁶H. E. Buckley, *Crystal Growth* (Wiley, New York, 1951), pp. 202–204.

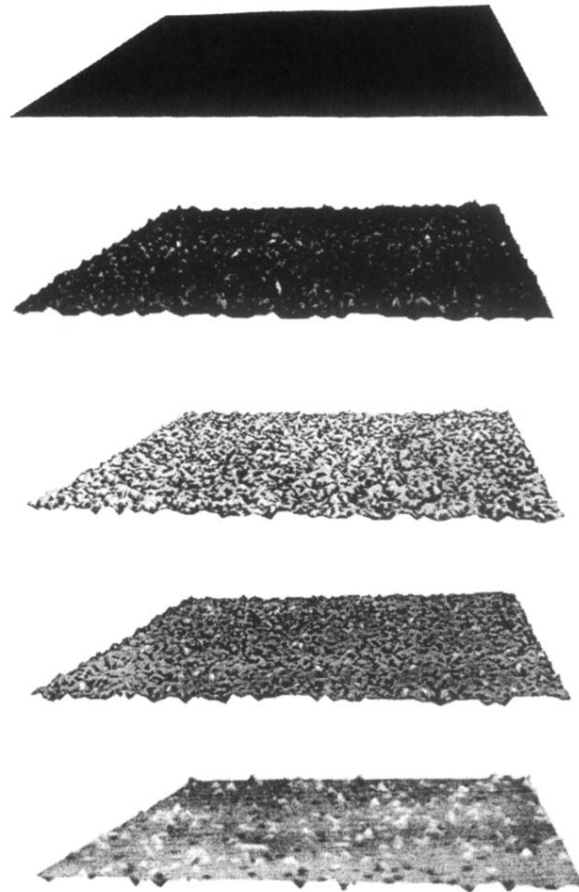


FIG. 5. Sequence of snapshots of a growing surface at different coverages (top to bottom) 0.0, 0.25, 0.50, 0.75, and 1.00. The simulation parameters are $L = 128$, $k_b T/J = 2.50$, and $\text{flux} = 10^{13}/\text{cm}^2 \text{sec}$. Lighter areas are at a greater height above the substrate than dark areas.

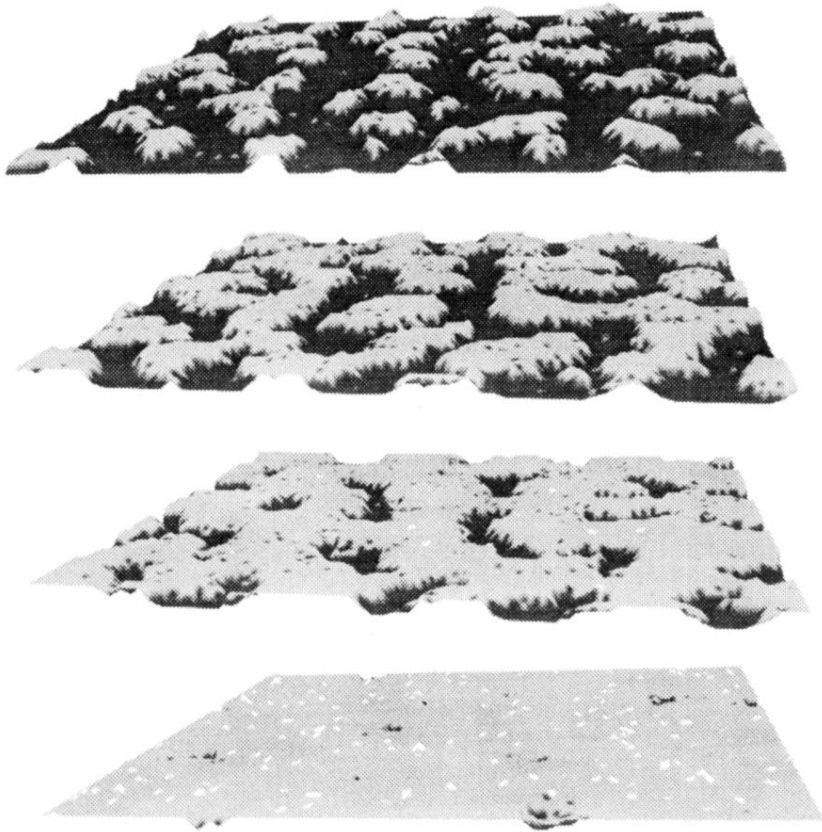


FIG. 6. Sequence of snapshots of growing surfaces for a much smaller flux than in Fig. 5 at coverages (top to bottom) 0.25, 0.50, 0.75, and 1.00. Simulation parameters are $L = 128$, $K_b T/J = 0.70$, and flux = $10^{10}/\text{cm}^2 \text{ sec}$.

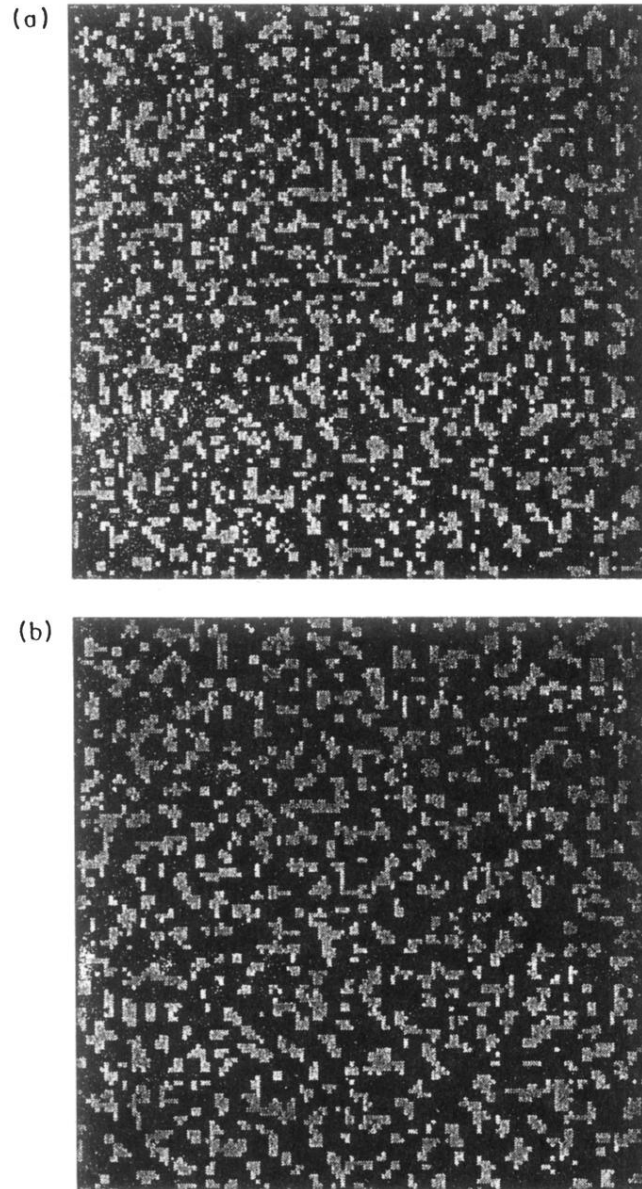


FIG. 7. (a) Surface growth at $k_b T/J=0.7$, flux $=5 \times 10^{12}/\text{cm}^2 \text{sec}$, and coverage of 0.25. Light areas indicate the adatoms. (b) The surface shown in this figure is first grown up to a coverage of 0.25 with the same simulation parameters as in (a). The flux is then turned off, and the surface is quenched to a temperature of $k_b T/J=0.5$. The picture shown here is taken 10 sec after the quenching.

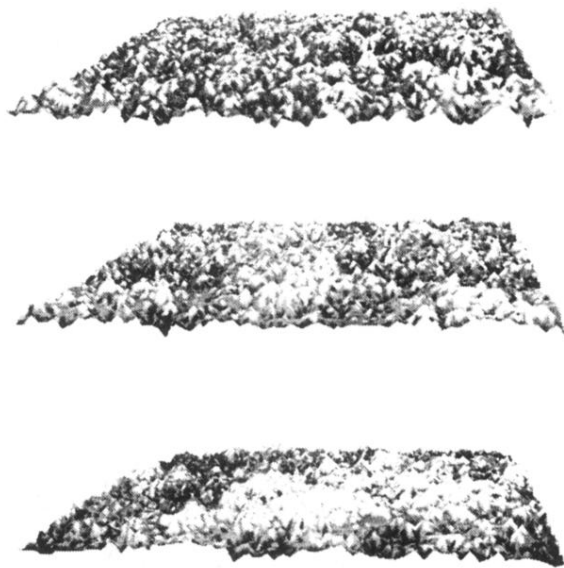


FIG. 8. Growth of surface fluctuations with time is shown in these pictures. The snapshots are taken at times (top to bottom) $t = 10, 20,$ and 600 sec. The interfacial width saturated around $t = 300$ sec. The lattice size is $L = 128,$ $k_b T/J = 1.70,$ and $\text{flux} = 10^{14}/\text{cm}^2 \text{ sec}.$